Electronic Supplementary Information for JAAS publication:

# Assessment of a simple partial LTE model for semi-quantitative ICP-OES analysis based on one single element calibration standard

**Joshua R. Dettman[a,b] and John W. Olesik*[,b]**

[a] *The Ohio State University, Department of Chemistry, 100 West 18th Avenue, Columbus Ohio, USA.*
[b] *The Ohio State University, School of Earth Sciences, 125 South Oval Mall, Columbus, Ohio, USA, Fax: 1 614 292 7688; Tel: 1 614 292 6954; E-mail: olesik.2@osu.edu*

**Table S1** Sources for energy levels and degeneracies.

| Element | Spectrum | Source | Element | Spectrum | Source | Element | Spectrum | Source | Element | Spectrum | Source |
|---|---|---|---|---|---|---|---|---|---|---|---|
| Ag | I | 1 | Eu | I | 2 | Nb | I | 3 | Sn | I | 1 |
| | II | 1 | | II | 2 | | II | 3 | | II | 1 |
| Al | I | 2 | Fe | I | 2 | Nd | I | 2 | Sr | I | 3 |
| | II | 2 | | II | 2 | | II | 2 | | II | 3 |
| As | I | 2 | Ga | I | 2 | Ni | I | 2 | Ta | I | 1 |
| | II | 2 | | II | 2 | | II | 2 | | II | 1 |
| Au | I | 1 | Gd | I | 2 | Os | I | 1 | Tb | I | 2 |
| | II | 1 | | II | 2 | | II | 1 | | II | 2 |
| B | I | 2 | Ge | I | 2 | P | I | 2 | Tc | I | 1 |
| | II | 2 | | II | 2 | | II | 2 | | II | 1 |
| Ba | I | 2 | Hf | I | 1 | Pb | I | 1 | Te | I | 1 |
| | II | 2 | | II | 1 | | II | 1 | | II | 1 |
| Be | I | 2 | Hg | I | 2 | Pd | I | 4 | Th | I | 5 |
| | II | 2 | | II | 2 | | II | 6 | | II | 5 |
| Bi | I | 1 | Ho | I | 2 | Pr | I | 2 | Ti | I | 2 |
| | II | 1 | | II | 2 | | II | 2 | | II | 2 |
| Br | I | 2 | I | I | 1 | Pt | I | 7 | Tl | I | 1 |
| | II | 2 | | II | 1 | | II | 8 | | II | 1 |
| Ca | I | 2 | In | I | 1 | Rb | I | 2 | Tm | I | 2 |
| | II | 2 | | II | 9 | | II | 2 | | II | 2 |
| Cd | I | 1 | Ir | I | 1 | Re | I | 1 | U | I | 5 |
| | II | 1 | | II | 10 | | II | 1 | | II | 5 |
| Ce | I | 2 | K | I | 2 | Rh | I | 1 | V | I | 2 |
| | II | 2 | | II | 2 | | II | 1 | | II | 2 |
| Cl | I | 2 | La | I | 2 | Ru | I | 1 | W | I | 2 |
| | II | 2 | | II | 2 | | II | 1 | | II | 2 |
| Co | I | 2 | Li | I | 2 | S | I | 2 | Y | I | 3 |
| | II | 2 | | II | 2 | | II | 2 | | II | 11 |
| Cr | I | 2 | Lu | I | 2 | Sb | I | 1 | Yb | I | 2 |
| | II | 2 | | II | 2 | | II | 1 | | II | 2 |
| Cs | I | 12 | Mg | I | 2 | Sc | I | 2 | Zn | I | 2 |
| | II | 13 | | II | 2 | | II | 2 | | II | 2 |
| Cu | I | 2 | Mn | I | 2 | Se | I | 2 | Zr | I | 3 |
| | II | 2 | | II | 2 | | II | 2 | | II | 3 |
| Dy | I | 2 | Mo | I | 2 | Si | I | 2 | | | |
| | II | 2 | | II | 2 | | II | 2 | | | |
| Er | I | 2 | Na | I | 2 | Sm | I | 2 | | | |
| | II | 2 | | II | 2 | | II | 2 | | | |

**Table S2** Subset of lines used for comparison of the pLTE and LTE model based semi-quantitative analysis.

| Element | Atom or ion | Wavelength (nm) | EP (eV) | IP (eV) | EP+IP (eV) |
|---|---|---|---|---|---|
| Na | I | 589.592 | 2.1 | 5.1 | 2.1 |
| Ca | I | 422.673 | 2.9 | 6.1 | 2.9 |
| Mg | I | 285.213 | 4.3 | 7.6 | 4.3 |
| Cd | I | 228.802 | 5.5 | 9.0 | 5.5 |
| Zn | I | 213.857 | 5.8 | 9.4 | 5.8 |
| Ba | II | 455.403 | 2.7 | 5.2 | 7.9 |
| Ca | II | 396.847 | 3.1 | 6.1 | 9.2 |
| Ca | II | 393.366 | 3.2 | 6.1 | 9.3 |
| Mg | II | 280.271 | 4.4 | 7.6 | 12.1 |
| Mg | II | 279.553 | 4.4 | 7.6 | 12.1 |
| Mn | II | 260.568 | 4.8 | 7.4 | 12.2 |
| Mn | II | 259.372 | 4.8 | 7.4 | 12.2 |
| Mn | II | 257.610 | 4.8 | 7.4 | 12.2 |
| Mn | II | 294.920 | 5.4 | 7.4 | 12.8 |
| Mn | II | 293.305 | 5.4 | 7.4 | 12.8 |
| Ca | II | 317.933 | 7.0 | 6.1 | 13.2 |
| Cd | II | 226.502 | 5.4 | 9.0 | 14.4 |
| Cd | II | 214.440 | 5.8 | 9.0 | 14.8 |
| Zn | II | 206.200 | 6.0 | 9.4 | 15.4 |
| Zn | II | 202.548 | 6.1 | 9.4 | 15.5 |

**Table S3** Semi-quantitative analysis results for Bi, Mo, Tl and Ga atom and ion lines and the impact of a small change in the fraction as ions.

| Emission line | IP/eV | pLTE model | | | Hypothetical adjusted % atoms | | |
|---|---|---|---|---|---|---|---|
| | | % ions 8200 K | % atoms 8200 K | Factor from correct | % ions 8200 K | % atoms 8200 K | Factor from correct |
| Bi I 222 | 7.3 | 89 | 11 | 16.6 | 98 | 2 | 3.0 |
| Bi I 223 | | | | 8.2 | | | 1.5 |
| Bi I 306 | | | | 2.9 | | | 0.5 |
| Bi II 190 | | | | 0.6 | | | 0.6 |
| *Bi I 195* | | | | 11.4 | | | 2.1 |
| *Bi I 289* | | | | 15.1 | | | 2.7 |
| *Bi I 211* | | | | 14.6 | | | 2.7 |
| *Bi I 293* | | | | 14.3 | | | 2.6 |
| *Bi I 298* | | | | 3.3 | | | 0.6 |
| Mo I 315 | 7.1 | 92 | 8 | 10.5 | 97.7 | 2.3 | 3.0 |
| Mo II 203 | | | | 1.7 | | | 1.8 |
| Mo II 204 | | | | 1.7 | | | 1.8 |
| Mo II 281 | | | | 0.9 | | | 1.0 |
| Mo II 202 | | | | 1.2 | | | 1.3 |
| *Mo I 313* | | | | 5.1 | | | 1.5 |
| *Mo I 317* | | | | 5.0 | | | 1.4 |
| *Mo I 379* | | | | 2.5 | | | 0.7 |
| *Mo I 386* | | | | 3.2 | | | 0.9 |
| Tl I 351 | 6.1 | 98 | 2 | 5.9 | 99.4 | 0.6 | 1.8 |
| Tl I 276 | | | | 4.7 | | | 1.4 |
| Tl II 190 | | | | 1.0 | | | 1.0 |
| *Tl I 377* | | | | 4.2 | | | 1.3 |
| *Tl I 237* | | | | 10.0 | | | 3.0 |
| *Tl I 291* | | | | 6.3 | | | 1.9 |
| *Tl I 258* | | | | 9.0 | | | 2.7 |
| *Tl I 352* | | | | 5.4 | | | 1.6 |
| Ga I 294 | 6.0 | 96 | 4 | 3.7 | 97.2 | 2.8 | 2.6 |
| Ga I 417 | | | | 2.6 | | | 1.8 |
| *Ga I 287* | | | | 3.2 | | | 2.3 |
| *Ga I 294* | | | | 4.3 | | | 3.0 |

Italics indicate additional lines from Boumans beyond the initial set of 261. Intensities are from Boumans[48]. pLTE temperature is estimated based on the Mg II 280/Mg I 285 nm emission intensity ratio. Mn I 279 nm sensitivity was empirically measured using 10 ppm Mn solution. Numbers in red indicate semi-quantitative concentrations that are more than a factor of three from correct concentrations.

**Table S4** The 122 emission lines which when used to empirically determine sensitivity for one element along with the pLTE model provide semi-quantitative concentration results for 63 elements that are within 3x of the correct value based on ≥86% of the 213 emission lines studied using Boumans[14] intensities.

| | λ (nm) | Atom or Ion | EP (eV) | IP (eV) | % within 3x* | | λ (nm) | Atom or Ion | EP (eV) | IP (eV) | % within 3x* | | λ (nm) | Atom or Ion | EP (eV) | IP (eV) | % within 3x* |
|---|---|---|---|---|---|---|---|---|---|---|---|---|---|---|---|---|---|
| Ag | 328.068 | I | 3.8 | 7.6 | 91% | Ge | 265.118 | I | 4.9 | 7.9 | 92% | Sb | 204.957 | I | 7.1 | 8.6 | 90% |
| Ag | 338.289 | I | 3.7 | 7.6 | 88% | Ge | 303.906 | I | 5.0 | 7.9 | 94% | Sc | 357.253 | II | 3.5 | 6.6 | 89% |
| Al | 309.271 | I | 4.0 | 6.0 | 90% | Hf | 277.336 | II | 5.3 | 6.8 | 93% | Sc | 336.127 | II | 3.7 | 6.6 | 88% |
| As | 193.696 | I | 6.4 | 9.8 | 92% | Hf | 264.141 | II | 5.7 | 6.8 | 90% | Se | 196.026 | I | 6.3 | 9.8 | 90% |
| Au | 242.795 | I | 5.1 | 9.2 | 94% | In | 230.606 | II | 5.4 | 5.8 | 93% | Si | 251.611 | I | 5.0 | 8.2 | 94% |
| B | 249.677 | I | 5.0 | 8.3 | 93% | In | 325.609 | I | 4.1 | 5.8 | 92% | Si | 288.158 | I | 5.1 | 8.2 | 90% |
| B | 249.772 | I | 5.0 | 8.3 | 93% | In | 303.936 | I | 4.1 | 5.8 | 92% | Si | 252.851 | I | 6.1 | 8.2 | 94% |
| B | 208.889 | I | 5.9 | 8.3 | 92% | La | 379.478 | II | 3.5 | 6.5 | 91% | Sm | 442.434 | II | 3.3 | 5.6 | 93% |
| Be | 313.107 | II | 4.0 | 9.3 | 94% | La | 407.735 | II | 3.3 | 6.5 | 93% | Sm | 388.529 | II | 3.7 | 5.6 | 92% |
| Be | 313.042 | II | 4.0 | 9.3 | 89% | Li | 670.784 | I | 1.8 | 5.4 | 92% | Sm | 428.079 | II | 3.4 | 5.6 | 94% |
| Ca | 317.933 | II | 7.1 | 6.1 | 93% | Li | 610.362 | I | 3.9 | 5.4 | 92% | Sn | 189.927 | I | 7.1 | 7.3 | 87% |
| Ca | 315.887 | II | 7.1 | 6.1 | 89% | Lu | 291.139 | II | 6.0 | 5.4 | 92% | Sr | 460.733 | I | 2.7 | 5.7 | 94% |
| Ce | 418.660 | II | 3.8 | 5.5 | 94% | Mg | 285.213 | I | 4.3 | 7.6 | 92% | Ta | 226.230 | II | 5.8 | 7.6 | 91% |
| Ce | 413.380 | II | 3.9 | 5.5 | 92% | Mg | 280.271 | II | 4.4 | 7.6 | 91% | Tb | 350.917 | II | 3.5 | 5.9 | 93% |
| Ce | 456.236 | II | 3.2 | 5.5 | 92% | Mg | 279.553 | II | 4.4 | 7.6 | 88% | Te | 214.281 | II | 5.8 | 9.0 | 87% |
| Ce | 394.274 | II | 4.0 | 5.5 | 92% | Mn | 294.92 | II | 5.4 | 7.4 | 91% | Th | 283.730 | II | 5.1 | 6.3 | 90% |
| Cd | 228.802 | I | 5.4 | 9.0 | 93% | Mn | 293.305 | II | 5.4 | 7.4 | 93% | Th | 283.231 | II | 4.9 | 6.3 | 90% |
| Cd | 214.440 | II | 5.8 | 9.0 | 93% | Mn | 279.482 | I | 4.4 | 7.4 | 94% | Th | 325.627 | II | 5.0 | 6.3 | 91% |
| Cd | 226.502 | II | 5.5 | 9.0 | 91% | Mn | 403.075 | I | 3.1 | 7.4 | 93% | Ti | 334.903 | II | 4.3 | 6.8 | 94% |
| Co | 228.616 | II | 5.8 | 7.9 | 93% | Mo | 202.031 | II | 6.1 | 7.1 | 93% | Tl | 190.801 | II | 6.5 | 6.1 | 94% |
| Co | 238.892 | II | 5.6 | 7.9 | 92% | Mo | 203.845 | II | 6.1 | 7.1 | 88% | Tm | 346.220 | II | 3.6 | 6.2 | 94% |
| Co | 236.380 | II | 5.7 | 7.9 | 90% | Mo | 204.597 | II | 6.1 | 7.1 | 87% | Tm | 324.154 | II | 3.8 | 6.2 | 91% |
| Co | 231.160 | II | 5.9 | 7.9 | 90% | Mo | 281.616 | II | 6.1 | 7.1 | 92% | Tm | 336.261 | II | 3.7 | 6.2 | 89% |
| Cr | 205.560 | II | 6.0 | 6.8 | 94% | Na | 589.592 | I | 2.1 | 5.1 | 93% | Tm | 384.802 | II | 3.2 | 6.2 | 91% |
| Cr | 283.563 | II | 5.9 | 6.8 | 92% | Na | 588.995 | I | 2.1 | 5.1 | 94% | U | 367.007 | II | 3.5 | 6.2 | 94% |
| Cr | 357.869 | I | 3.5 | 6.8 | 90% | Nd | 430.358 | II | 2.9 | 5.5 | 87% | U | 409.014 | II | 3.3 | 6.2 | 88% |
| Cr | 206.158 | II | 6.0 | 6.8 | 93% | Ni | 231.604 | II | 6.4 | 7.6 | 92% | V | 290.880 | II | 4.7 | 6.7 | 94% |
| Dy | 394.468 | II | 3.1 | 5.9 | 92% | Ni | 232.003 | I | 5.3 | 7.6 | 92% | V | 270.093 | II | 4.6 | 6.7 | 92% |
| Er | 337.271 | II | 3.7 | 6.1 | 89% | Ni | 341.476 | I | 3.7 | 7.6 | 89% | W | 224.876 | II | 5.5 | 7.9 | 92% |
| Er | 349.910 | II | 3.6 | 6.1 | 87% | Pb | 283.306 | I | 4.4 | 7.4 | 90% | W | 239.708 | II | 5.6 | 7.9 | 93% |
| Er | 339.200 | II | 3.7 | 6.1 | 93% | Pb | 405.781 | I | 4.4 | 7.4 | 93% | W | 248.923 | II | 5.6 | 7.9 | 94% |
| Eu | 381.967 | II | 3.3 | 5.7 | 87% | Pd | 248.892 | II | 8.1 | 8.3 | 94% | Yb | 289.138 | II | 4.3 | 6.3 | 89% |
| Fe | 238.204 | II | 5.2 | 7.9 | 89% | Pr | 390.844 | II | 3.2 | 5.5 | 91% | Zn | 206.200 | II | 6.0 | 9.4 | 90% |
| Fe | 239.562 | II | 5.2 | 7.9 | 92% | Pr | 414.311 | II | 3.4 | 5.5 | 89% | Zn | 213.857 | I | 5.8 | 9.4 | 92% |
| Fe | 259.939 | II | 4.8 | 7.9 | 91% | Pr | 422.293 | II | 3.0 | 5.5 | 92% | Zn | 202.548 | II | 6.1 | 9.4 | 92% |
| Fe | 238.863 | II | 5.2 | 7.9 | 93% | Pt | 265.945 | I | 4.7 | 9.0 | 93% | Zr | 343.823 | II | 3.7 | 6.6 | 91% |
| Gd | 342.247 | II | 3.9 | 6.2 | 94% | Pt | 299.797 | I | 4.2 | 9.0 | 91% | Zr | 257.139 | II | 4.9 | 6.6 | 90% |
| Gd | 336.223 | II | 3.8 | 6.2 | 93% | Re | 227.525 | II | 5.4 | 7.8 | 93% | Zr | 357.685 | II | 3.9 | 6.6 | 92% |
| Gd | 335.047 | II | 3.8 | 6.2 | 94% | Ru | 349.894 | I | 3.5 | 7.4 | 92% | | | | | | |

*fraction of 213 emission lines that produce semi-quantitative concentrations within 3x of the correct value.

**Table S5** Semi-quantitative concentrations factor from correct concentration for emission lines not listed in Boumans[14] tables.

| | | Wavelength (nm) | Factor from correct conc. |
|---|---|---|---|
| B | I | 182.528 | 0.4 |
| B | I | 182.578 | 0.9 |
| Hg | II | 194.168 | 24 |
| Hg | I | 184.886 | 4.0 |
| Hg | I | 546.074 | 73 |
| I | I | 178.215 | 0.8 |
| I | I | 182.976 | 3.3 |
| K | I | 766.490 | 2.3 |
| K | I | 404.721 | 206 |
| P | I | 178.221 | 0.5 |
| P | I | 177.434 | 0.1 |
| Rb | I | 780.023 | 1.6 |
| Zr | II | 354.262 | 1.1 |
| Zr | II | 357.247 | 1.0 |

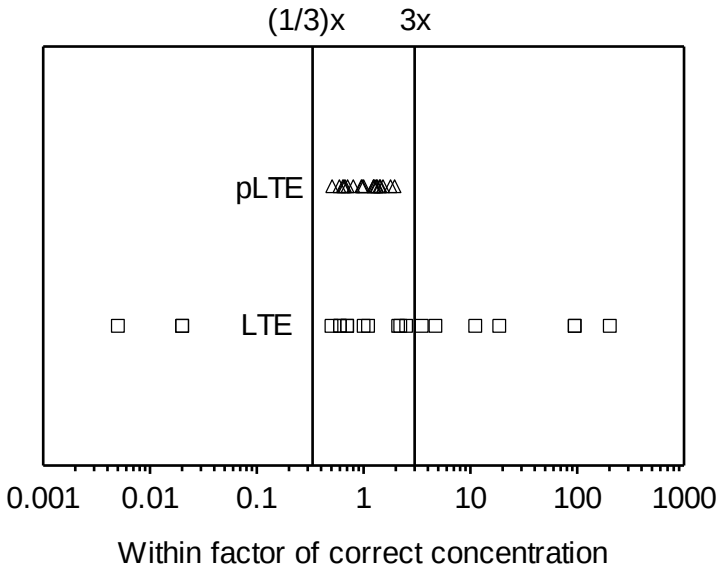


**Figure S1** Semi-quantitative concentration divided by actual concentration for 7 elements based on 20 emission lines using LTE and pLTE models. Intensities are from Boumans[14], temperature is estimated based on the Mg II 280/Mg I 285 intensity ratio. The standard solution contained 10 ppm Mg. The Mg I 285 nm sensitivity was determined empirically.

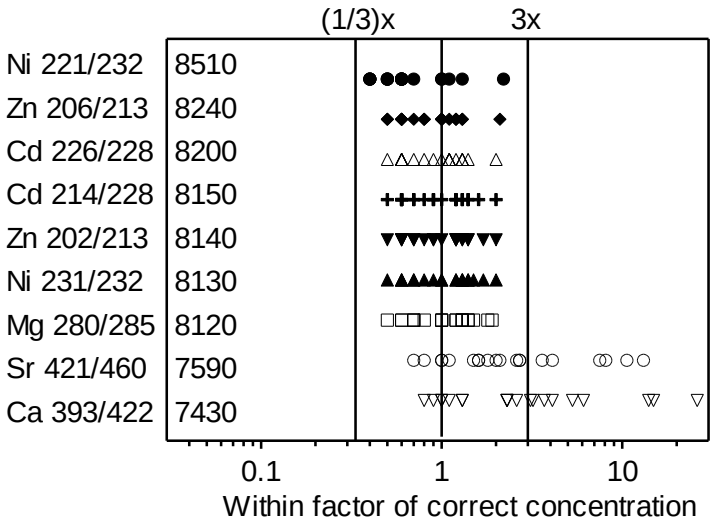


**Figure S2** Semi-quantitative concentration divided by actual concentration when different ion and atom lines pairs were used to determine temperature. Intensities are from Boumans[14]. The standard solution contained 10 ppm Mg. The Mg I 285 nm sensitivity was determined empirically, independent of the pLTE model.

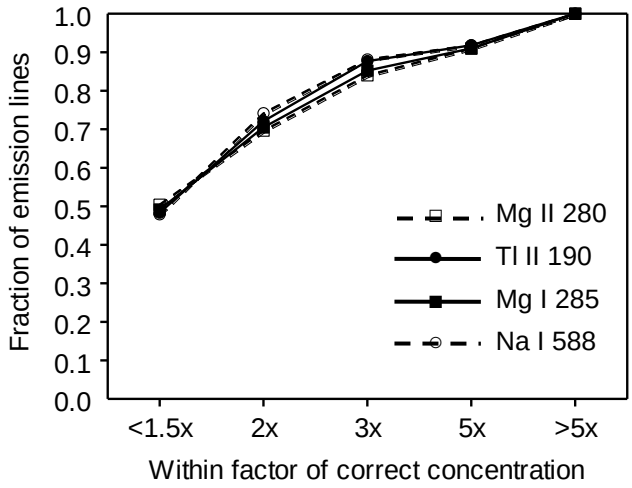


**Figure S3** Fraction of 231 emission lines versus semi-quantitative concentrations divided by actual concentrations of 63 elements. Four different lines from a standard of known concentration Mg, Tl, or Na were used to calculate sensitivity for one line. Intensities are from Boumans[14]. Temperature is estimated based on the Mg II 280/Mg I 285 nm emission intensity ratio.

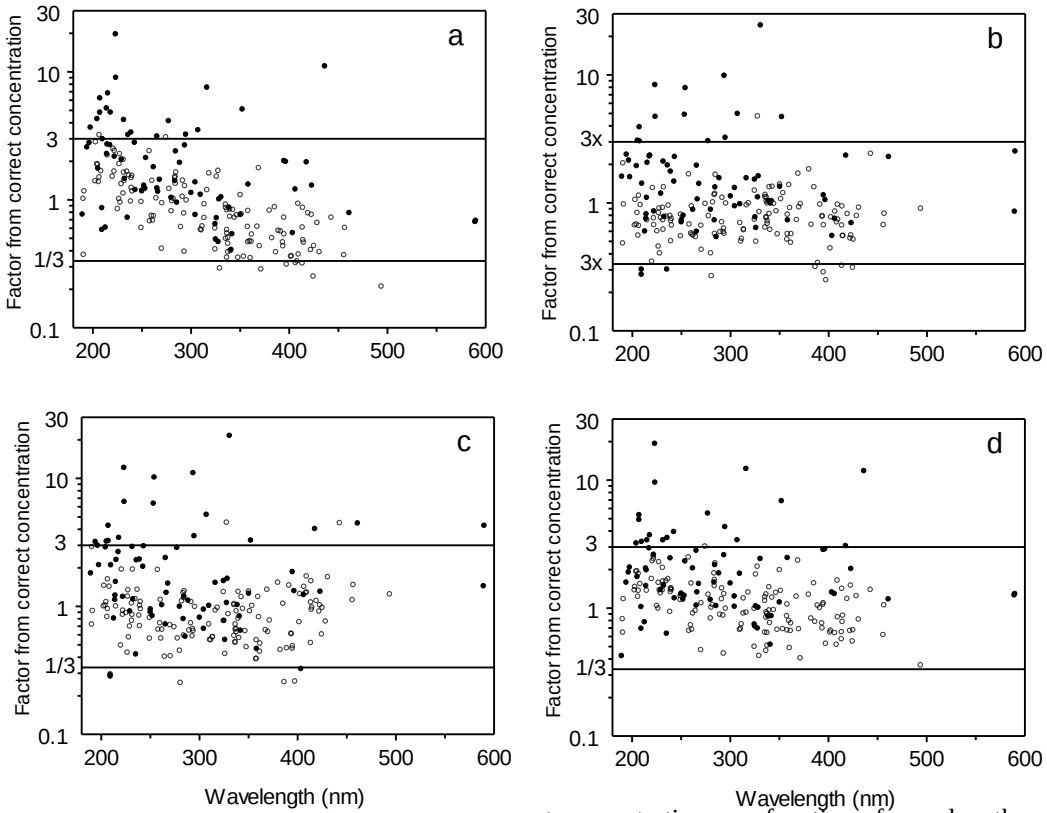


**Figure S4** Semi-quantitative concentration factor from correct concentration as a function of wavelength. **a.** From Optima 5300V, Optima/Boumans intensity ratios to estimate spectrometer response. **b.** From Optima 5300V, spectrometer response calculated from transmission of individual optical components. **c.** From Optima 5300V, intensities without correction for spectrometer response. **d.** From Boumans[14]. pLTE temperature determined from Mg II 280 nm/Mg I 285 nm emission intensity ratio. Mn II 294 sensitivity determined from 10 ppm Mn solution. ●: atom lines, ○: ion lines. All cases the ratio of continuum background intensities used to determine spectrometer response for the wavelengths of the ion/atom line pair used to determine pLTE temperature.

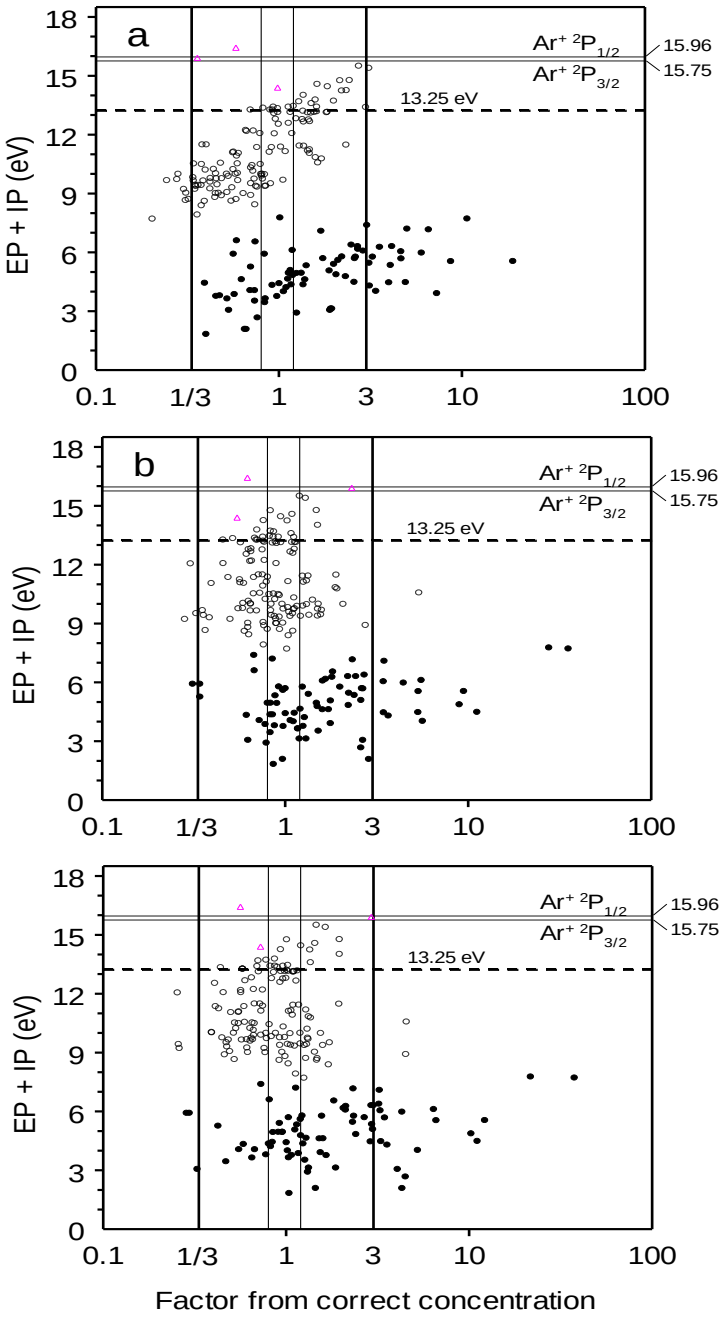


**Figure S5** Factor semi-quantitative concentrations (based on Optima 5300V intensities) were from correct concentration. Wavelength dependent spectrometer response determined from: **a.** Ratio of Boumans/Optima 5300V ICP-OES intensities (pLTE temperature: 8100 K), **b.** Individual optical component light transfer efficiencies. Temperature is estimated based on the Mg II 280/Mg I 285 intensity ratio. Mn I 279 nm sensitivity determined from 10 ppm Mn solution. ○: ion lines, ●: atom lines. △: lines with excitation plus ionization energies greater than 13.25 eV with spin forbidden charge transfer reactions.

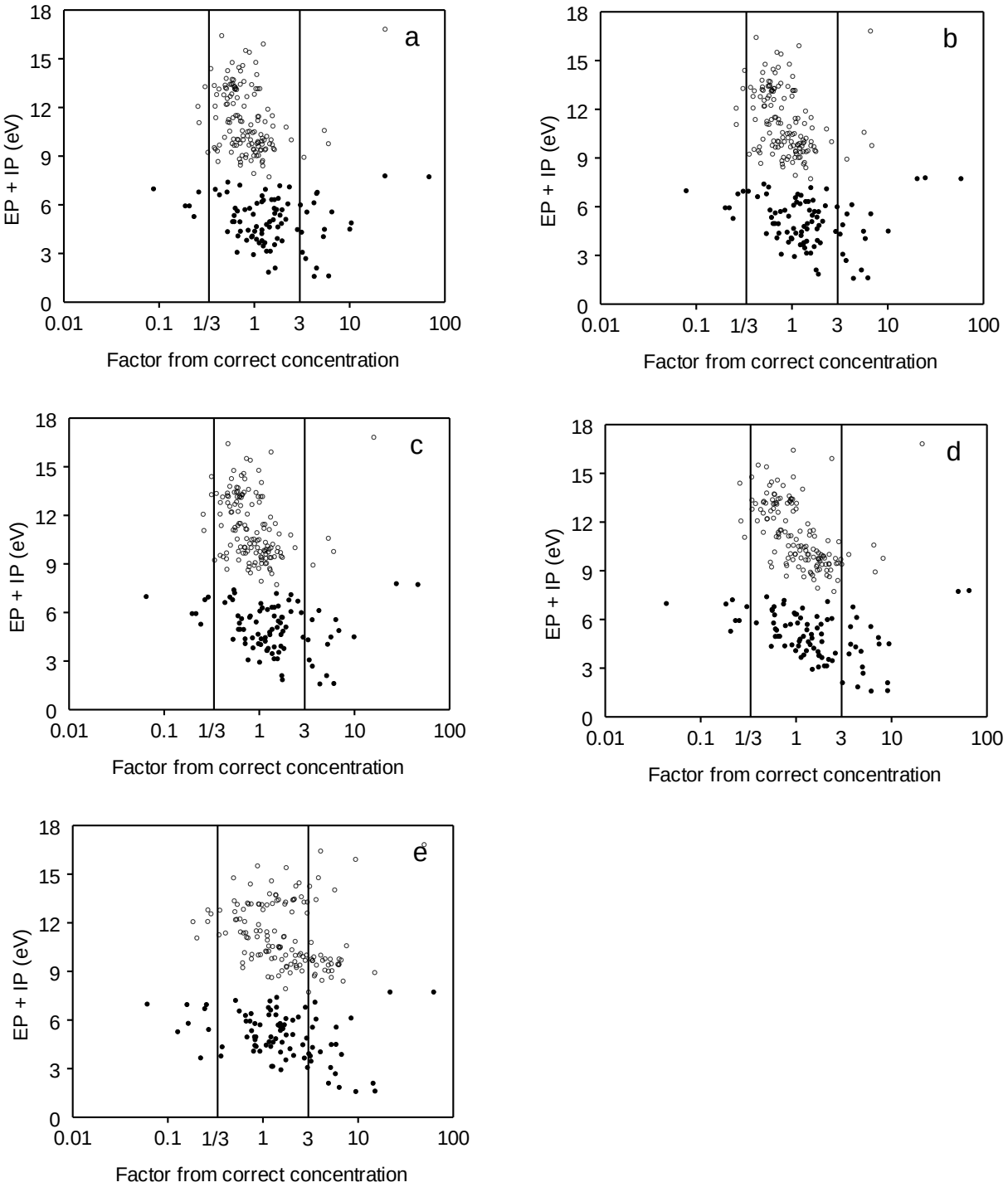


**Figure S6** Comparison of semi-quantitative concentration accuracy for 66 elements based on 227 emission lines under different operating conditions (a-e). Operating conditions listed in Table 14. Emission intensities are experimentally measured and corrected for wavelength dependent spectrometer response based on individual optical components. Temperature estimated based on the Mg II 280/Mg I 285 emission intensity ratio. Mn II 294 nm sensitivity was determined from a 10 ppm Mn solution ○: ion lines, ●: atom lines.

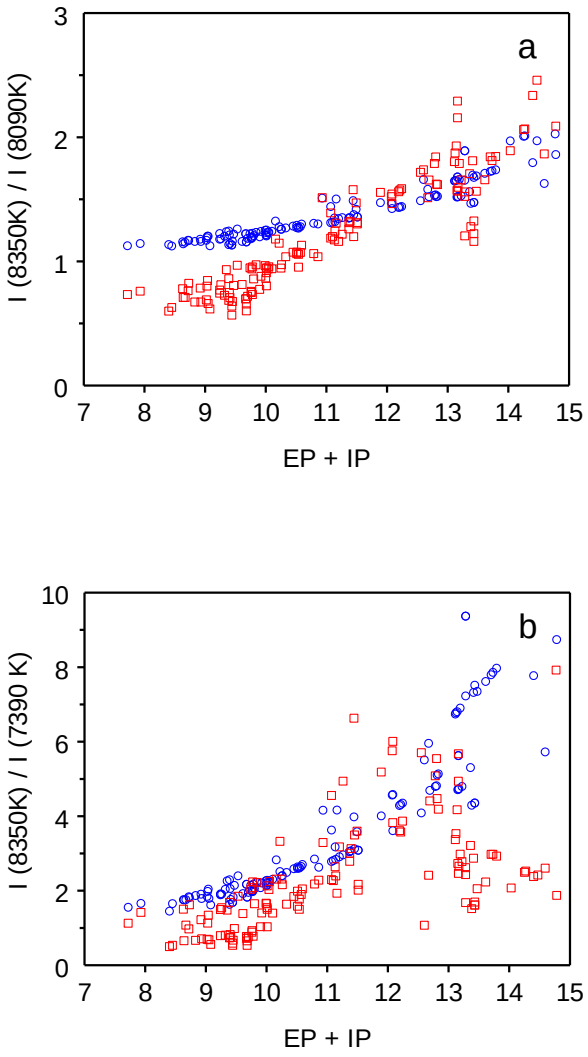


**Figure S7** Ratio of ion line intensities as a function of the sum of excitation and ionization energies. **a.** Intensity at 8350 K / Intensity at 8090 K. **b.** Intensity at 8350 K / Intensity at 7390 K. ○: pLTE □: experimental.

## Appendix S1 Calculation of %excited,i and %ions from the Boltzmann and Saha distributions

For a plasma in LTE, the percentage of analyte ions (or atoms) in a particular excited level i (%excited,i in eqn (1)) is determined by the Boltzmann excitation distribution

$$\%\,\text{excited, i} = \frac{g_i}{Z_M(T)} 10^{-5040 EP_i / T} \tag{S1}$$

where $g_i$, is the degeneracy of level I, $Z_M$ is the partition function, $EP_i$ is the excitation potential of level i, and T is the plasma temperature. Under LTE conditions the Saha-Boltzmann equation relates the level populations of ion level p and atom level o is:

$$\frac{n_{M^+,p}}{n_{M,o}} = 4.83 \text{x} 10^{15} \frac{g_{M^+p}}{g_{M,o}} \frac{T^{3/2}}{n_e} e^{(EP_{M,o} - IP - EP_{M^+,p})/kT} \tag{S2}$$

The LTE model does not include radiative recombination. In the pLTE approach, the highly excited atom and ground ion levels are assumed to be in LTE with each other. This allows the ionization equilibrium to be calculated based on the ion ground level and the highest energy atom level using the LTE based Saha-Boltzmann equation without assuming the presence or absence of radiative recombination. When p is the ion ground level and o is the highest energy atom level, the exponent in eqn (14) is ~0 and the resulting equation is called the Saha jump.

$$\text{Saha jump} = \left( \frac{n_{M^+,\text{groundstate}}}{n_{M,\text{highestatom}}} \right)_{LTE} = 4.83 \text{x} 10^{15} \frac{g_{M^+,p}}{g_{M,o}} \frac{T^{3/2}}{n_e} \tag{S3}$$

The populations of all atom levels are multiplied by the Saha atom scaling factor

$$\text{Saha atom scaling factor} = \frac{n_{M^+,\text{groundstate}}}{n_{M,\text{highestatom}} \times \text{Saha jump}} \tag{S4}$$

Then the %ions is calculated by dividing the sum of the relative populations of all ion levels by the sum of the populations of all atom and ion levels. The %atoms is 1-%ions.

## Appendix S2 Calculation of electron number density from temperature

Level populations were calculated over a temperature range of 7000 to 10,000 K in 10 K increments. The equations for $b_i$ are also dependent on $n_e$ making it necessary to estimate $n_e$ at each temperature used for modeling. By assuming the only source of electrons is the plasma gas Ar, the $n_e$ that corresponds to each plasma temperature can be calculated. If the plasma is overall neutral ($n_e = n_{Ar}+$) the Saha equation becomes

$$S(T) = \frac{n_e n_{Ar^+}}{n_{Ar}} = \frac{{n_e}^2}{n_{Ar}} \tag{S5}$$

In using the Saha equation we assume that Ar is in LTE. This may be a reasonable assumption for Ar as the radiative de-excitation not included in the LTE model may be at least partially balanced by re-absorption of emission before it exits the plasma.[15,16]. Dalton's Law of partial pressures relates the number density of ground level Ar to pressure and temperature, assuming that virtually all Ar is in the ground level (very small percentage of Ar is excited or exists as $Ar^+$)

$$P = kT\Sigma n = kTn_{Ar} \tag{S6}$$

where k is the Boltzmann constant. Thus

$$n_e^2 = S(T)\frac{P}{kT} \quad \text{(S7)}$$

With pressure = 1 atm and temperature in K

$$n_e^2 = 4.83x10^{15}\frac{Z_{Ar^+}(T)}{Z_{Ar}(T)}10^{-5040\,ArIP/T}\frac{7.34x10^{21}}{T} \quad \text{(S8)}$$

$Z_{Ar} = g_{atom,\,gs} = 1$ and $Z_{iAr}+ = 5.5$ ($Z_{ion}$ varies from 5.49 to 5.62 from 7000 to 10,000 K[17]) were used. The equation above allows for the calculation of electron number density due to ionization of Ar from temperature.

## Appendix S3 Summary of level population calculation procedure at a single plasma temperature

1 Input first ionization energy and level energies and degeneracies for atom and singly charged ion into MATLAB.
2 At a given temperature calculate relative populations of atom levels using the Boltzmann distribution. Repeat for ion levels.
3 Use Saha jump to set ion to atom equilibrium based on last atom level and ion ground level. Multiply all atom populations by the Saha atom scaling factor.
4 Determine the fraction of atoms and ions in each level by dividing by the partition function calculated by summing the relative populations of all of the atom and ion levels. ($(\Sigma n_{atom,LTE} + \Sigma n_{ion,LTE}$ to 1).
5 Multiply atom and ion populations by $b_i$.
6 Normalize $\Sigma n_{atom,pLTE} + \Sigma n_{ion,pLTE}$ to 1. Populations in each level will be then expressed as fraction in each level.
7 Using Einstein A transition probabilities for the emission lines of interest and the fraction in the upper state involved in the transition, calculate sensitivity of emission lines of elements of interest in samples relative to the emission line of the element in the single element calibration standard. Convert relative sensitivities from molar basis to ppm basis.

## Appendix S4 Derivation of collisional de-excitation rate co-efficient $k_{CD}$ and discussion of differences from Burton and Blades $b_i$

The rate coefficient for collisional excitation, $k_{CE}$, will be derived here because Seaton[18] and Griem[19] give cross sections for excitation but not de-excitation. The collisional de-excitation rate coefficient $k_{CD}$ is related to $k_{CE}$.

Consider a closed system containing $n_e$ electrons per $cm^3$ moving at speed v (in cm/s) in a gas of $n_j$ ground level or excited atoms or ions per $cm^3$. Assume that the speed of electrons is much greater than the speed of atoms or ions such that the atoms or ions can be considered stationary. (At 8000 K the most probable speed for free electrons is 40x greater than H atoms disregarding the effect of the oscillating magnetic field used to sustain the plasma.) If $\sigma(v)$ (in $cm^2$) is the cross section for a particular transition at this electron speed v the rate of collisions with electrons is

$$CE = \sigma(v)\,v\,n_e\,n_j \quad \text{(S9)}$$

in $cm^{-3}\,s^{-1}$. Because the electrons in the ICP have a distribution of speeds,[20] eqn (20) becomes

$$CE = <\sigma(v)f(v)>\,n_e\,n_j \quad \text{(S10)}$$

f(v) is the Maxwell-Boltzmann speed probability density function

$$f(v) = 4\pi v^2 \left( \frac{m_e}{2\pi kT} \right)^{3/2} e^{(-m_e v^2 / 2kT)} \tag{S11}$$

where $m_e$ is the mass of an electron, v is electron speed, k is the Boltzmann constant, and T is temperature. The rate coefficient for collisional excitation is

$$k_{CE} = <\sigma(v) f(v)> = \int_{v=(2\Delta E/m)^{1/2}}^{\infty} \sigma(v) f(v) dv \tag{S12}$$

A conceptual plot is shown in Fig. S4, ESI†, the area under σ(v) x f(v) vs electron kinetic energy is $k_{CE}$.

It is impossible to measure cross sections for all possible transitions and an average analytic formula for cross sections is needed (cf.[21,22] for experimental methods of cross section measurement.) A formula for the average cross section for an excitation induced by collision with an electron is given by van Regemorter.[23] Similar formulae were obtained by Griem[19] and Seaton.[18]

$$\sigma(v) = \frac{8\pi}{\sqrt{3}} \frac{IH}{k_i^2 \Delta E} f_{ji} \bar{g} a_0^2 \tag{S13}$$

The symbols are identified in the Symbols section. The Gaunt factor is an empirical correction[18] that accounts for the fact that not every collision with greater than the threshold energy induces a transition as well as inaccuracies in the theoretical formula.[23] Thus $k_{CE}$ is

$$k_{CE} = \frac{3.64 x 10^{-13} A_{ij} < g >}{\Delta E^3 (kT)^{1/2}} \frac{g_i}{g_j} e^{\frac{-\Delta E_{ij}}{kT}} \tag{S14}$$

where the transition energy ΔE is in eV. The collisional de-excitation rate coefficient can be calculated from $k_{CE}$ using[24]

$$k_{CD} = k_{CE} \frac{g_j}{g_i} e^{\frac{\Delta E_{ij}}{kT}} \tag{S15}$$

$$k_{CD} = \frac{3.64 x 10^{-13} A_{ij} < g >}{\Delta E^3 (kT)^{1/2}} \tag{S16}$$

Burton and Blades reference Seaton[18] for their $k_{CD}$ which contains only a collisional de-excitation cross section σ(v) related to $k_{CD}$ as described above. They give no mention of assumptions made or further details about the process to derive $k_{CD}$ from σ(v).

$$k_{CD,Burton-Blades} = \frac{3.64 x 10^{-13} A_{ij} < g >}{E P_i \Delta E^2 (kT)^{1/2}} \tag{S17}$$

Our formula for $k_{CD}$ was derived[23]. Instead of $\Delta E^3$ Burton and Blades have $EP_i\Delta E^2$. In addition, the fit to <g> vs. $\Delta E/kT$ for atoms poorly matches the data in Elton and our fit in eqn (9).[25]

$$< g >_{\text{Burton–Blades}} = 0.114\left(\frac{\Delta E}{kT}\right)^{-0.607} \qquad \text{(S18)}$$

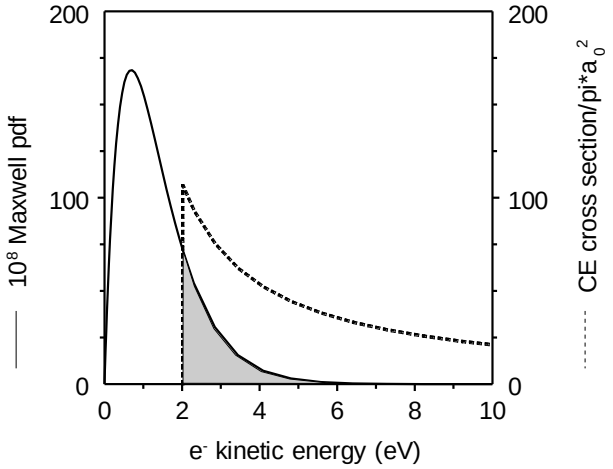


**Figure S6** Maxwell-Boltzmann probability density function ( ——— ) (eqn S11) and collisional excitation cross section ( – – – – ) (eqn S14) in units of geometric cross section ($\pi a_0^2$) as a function of colliding electron kinetic energy. In this example the transition has an energy of 2eV and a spontaneous emission probability of $10^8$/s. The collisional excitation rate coefficient $<\sigma(v)f(v)>$ or $k_{CE}$ is the shaded area under the curve. Note that the y axis of the plot on the right has been re-scaled for illustration purposes.

## Appendix S5 Calculation of wavelength independent light transfer efficiency for UV and visible channels of cross dispersed echelle spectrometer

Optical components after the echelle grating are different for the UV channel than the visible channel. Approximately two thirds of the light is intersected by the Schmidt cross disperser to the UV channel.[26] Wavelength independent transmission through the UV channel includes: reflectance off the UV camera sphere mirror (0.85 transmission), fold flat mirror (0.85), reflectance off the field flattener lens front (0.94) and rear surface (0.94) and internal transmission (the lens is thin, assume 1.00) through the field flattener lens. The net UV wavelength independent relative efficiency is 0.67 x 0.85 x 0.85 x 0.94 x 1.00 x 0.94 = 0.43.

One-third of the light passes through the Schmitt cross disperser to the visible channel. In addition, there is reflectance off the surfaces of two mirrors (0.94 transmission at each surface) and internal transmittance (0.92, assumed to be wavelength independent) through the prism, reflectance off three surfaces the compound lens (0.94 at each surface) and internal transmittance (lenses are thin, assume 0.92 total) through the two fused compound lenses, and reflectance off two surfaces of the field lens (0.94 at each surface) and internal transmittance (0.92) through the field lens. The net visible wavelength independent relative efficiency = 0.33 x 0.94 x 0.92 x 0.94 x 0.94 x 0.94 x 0.94 x 0.92 x 0.94 x 0.94 x 0.92 = 0.17.

## Symbols

| | |
|---|---|
| %excited,i | percentage of analyte ions in the plasma observation volume that are in the excited state corresponding to the upper level of the transition that produces light at wavelength $\lambda_i$, |
| %ions | percentage of atoms in the original sample that are converted into elemental ions in observation volume of the plasma |
| %light | percentage of light emitted that reaches the detector |
| $a_0$ | Bohr radius = $5.29 \times 10^{-11}$ m |
| $A_{ij}$ | Einstein spontaneous emission rate ($s^{-1}$) |
| $\alpha$ | Fine structure constant = 1/137 (unit less) |
| AW | Atomic weight (g/mol) |
| $b_i$ | Ratio of pLTE and LTE populations (unit less) |
| c | Speed of light (m/s) |
| CD | Rate of collision de-excitation ($s^{-1}$) |
| CE | Rate of collisional excitation ($s^{-1}$) |
| cf | factor to convert moles to atoms, grams to nanograms and mL/min to mL/s |
| ds | number of counts per photon produced by the detector |
| $\Delta E$ | Energy difference between level i and ion ground state (eV) |
| EP | Excitation potential (eV) |
| $f_{ji}$ | Absorption oscillator strength (unit less) |
| f(v) | Maxwell probability density function (unit less) |
| g | Degeneracy (unit less) |
| <g> | Thermally averaged Gaunt factor (unit less) |
| $\bar{g}$ | Gaunt factor (unit less) |
| $\hbar$ | Planck's constant/$2\pi$ = $1.055 \times 10^{-34}$ J·s |
| IP | Ionization potential (eV) |
| $IP_H$ | Ionization potential of hydrogen = 13.598 eV |
| k | Boltzmann constant = $8.65 \times 10^{-5}$ eV/K |
| $k_i$ | Initial electron kinetic energy (eV) |
| $k_{CD}$ | Collisional de-excitation rate coefficient ($cm^{-3}$ $s^{-1}$) |
| $k_{CE}$ | Collisional excitation rate coefficient ($cm^{-3}$ $s^{-1}$) |
| $\lambda$ | Wavelength (m) |
| $m_e$ | Mass of electron = $9.109 \times 10^{-31}$ kg |
| $n_e$ | Electron number density ($cm^{-3}$) |
| P | Pressure (atm) |
| RD | Rate of radiative de-excitation ($s^{-1}$) |
| $\sigma(v)$ | Cross section ($cm^2$) |
| S(T) | Saha distribution |
| t | time each analyte ion spends in the observation volume (s) |
| T | Temperature (K) |
| TR | Transport rate (atoms/s) |
| U | Sample uptake rate (mL/min) |
| $v_e$ | Electron speed (m/s) |
| Z(T) | Partition function (unitless) |

## References


1. C.E. Moore, "Atomic Energy Levels, Vol III, Circular of the National Bureau of Standards 467," (National Bureau of Standards, Washington D.C., 1958).
2. Y. Ralchenko, A. E. Kramida and J. Reader, NIST Atomic Spectra Database V. 3.1.5, <http://physics.nist.gov/asd3>, Accessed, 1-25-2010.
3. C.E. Moore, "Atomic Energy Levels, Vol II, Circular of the National Bureau of Standards 467," (National Bureau of Standards, Washington D.C., 1952).
4. R. Engelman, U. Litzen, H. Lundberg and J.F. Wyart, *Physica Scripta*, 1998, **57**, 345-364.
5. J. Blaise and J.F. Wyart, Selected Constants, Energy Levels, and Atomic Spectra of Actinides, <http://www.lac.u-psud.fr/Database/Contents.html> Accessed, 1-25-2010.
6. H. Lundberg, U. Litzen and S. Johansson, *Physica Scripta*, 1994, **50**, 110-118.
7. J. Blaise, J. Verge and J.F. Wyart, *J. Res. of the NIST*, 1992, **97**, 213-216.
8. J. Blaise, J. Verge and J.F. Wyart, *J. Res. of the NIST*, 1992, **97**, 217-223.
9. H. Karlsson and U. Litzen, *J. Phys. B: At. Mol. Opt. Phys.*, 2001, **34**, 4475-4485.
10. J. E. Sansonetti, W. C. Martin and S. L. Young, Handbook of Basic Atomic Spectroscopic Data, <http://www.nist.gov/physlab/data/handbook/index.cfm>, Accessed, 1-25-2010.
11. A.E. Nilsson, S. Johansson and R.L. Kurucz, *Physica Scripta*, 1991, **46**, 226-257.
12. K.H. Weber and J.E. Sansonetti, *Phys. Rev. A*, 1987, **35**, 4650-4660.
13. C.J. Sansonetti and K.L. Andrew, *J. Opt. Soc. Am. B*, 1986, **3**, 386-397.
14. P. W. J. M. Boumans, "Line Coincidence Tables for Inductively Coupled Plasma Atomic Emission Spectrometry," (Pergamon Press, Oxford, 1984).
15. J.W. Mills and G.M. Hieftje, *Spectrochim. Acta Part B*, 1984, **39**, 859-866.
16. M.W. Blades and G.M. Hieftje, *Spectrochim. Acta Part B*, 1982, **37**.
17. S. Tamaki and T. Kuroda, *Spectrochim. Acta Part B*, 1987, **42**, 1105-1111.
18. M. J. Seaton, in *Atomic and Molecular Processes*, ed. D. R. Bates, Academic Press, New York. 1962, pp. 414-417.
19. H.R. Griem, in *Plasma Spectroscopy*, McGraw-Hill, New York. 1964, pp. 130-150.
20. M. Huang, P. Y. Yang, D. S. Hanselman, C. A. Monnig and G. M. Hieftje, *Spectrochim. Acta Part B*, 1990, **45**, 511-520.
21. H. Massey, E. Burhop and H. Gilbody, "Electronic and Ionic Impact Phenomena," (Oxford University Press, London, 1969).
22. H. J. Kunze, *Space Sci. Rev.*, 1972, **13**, 565-583.
23. H. van Regemorter, *Astrophys J.*, 1962, **136**, 906-915.
24. I.I. Sobel'man, L.A. Vainshtein and E.A. Yukov, "Excitation of Atoms and Broadening of Spectral Lines," (Springer, Berlin, 1995). 7.
25. R.C. Elton, in *Methods of Experimental Physics*, ed. H. R. Griem and R. H. Lovenberg, Academic Press, New York, pp. 115-168.
26. B. Rasmussen, Personal communication, 2010.